2018

Autophagy regulates DUOX1 localization and superoxide production in airway epithelial cells during chronic IL-13 stimulation

John D. Dickinson
University of Nebraska at Omaha

Jenea M. Sweeter
University of Nebraska at Omaha

Kristi J. Warren
University of Nebraska at Omaha

Iman M. Ahmad
University of Nebraska at Omaha

Xavier De Deken
Universite Libre de Bruxelles

See next page for additional authors

Redox Biology 14 (2018) 272–284

Contents lists available at ScienceDirect

Redox Biology

journal homepage: www.elsevier.com/locate/redox

Autophagy regulates DUOX1 localization and superoxide production in airway epithelial cells during chronic IL-13 stimulation

John D. Dickinson[a,*], Jenea M. Sweeter[a], Kristi J. Warren[a], Iman M. Ahmad[b], Xavier De Deken[c], Matthew C. Zimmerman[d,1], Steven L. Brody[e,1]

[a] Pulmonary, Critical Care, Sleep and Allergy Division, Department of Internal Medicine, University of Nebraska Medical Center, Omaha, NE, USA
[b] Department of Medical Imaging and Therapeutic Sciences, College of Allied Health Professions, University of Nebraska Medical Center, Omaha, NE, USA
[c] Institut de Recherche Interdisciplinaire en Biologie Humaine et Moléculaire, Université libre de Bruxelles, Brussels, Belgium
[d] Department of Cellular and Integrative Physiology, University of Nebraska Medical Center, Omaha, NE, USA
[e] Department of Medicine, Washington University School of Medicine, Saint Louis, MO, USA

ARTICLE INFO

Keywords:
Asthma
Autophagy
DUOX1
Epithelial cells
IL-13
IL-4
Electron Paramagnetic Resonance Spectroscopy
Reactive oxygen species
Superoxide

ABSTRACT

The airway epithelium is a broad interface with the environment, mandating well-orchestrated responses to properly modulate inflammation. Classically, autophagy is a homeostatic pathway triggered in response to external cellular stresses, and is elevated in chronic airway diseases. Recent findings highlight the additional role of autophagy in vesicle trafficking and protein secretion, implicating autophagy pathways in complex cellular responses in disease. Th2 cytokines, IL-13 and IL-4, are increased in asthma and other airway diseases contributing to chronic inflammation. Previously, we observed that IL-13 increases reactive oxygen species (ROS) in airway epithelial cells in an autophagy-dependent fashion. Here, we tested our hypothesis that autophagy is required for IL-13-mediated superoxide production *via* the NADPH oxidase DUOX1. Using a mouse model of Th2-mediated inflammation induced by OVA-allergen, we observed elevated lung amounts of IL-13 and IL-4 accompanied by increased autophagosome levels, determined by LC3BII protein levels and immunostaining. ROS levels were elevated and DUOX1 expression was increased 70-fold in OVA-challenged lungs. To address the role of autophagy and ROS in the airway epithelium, we treated primary human tracheobronchial epithelial cells with IL-13 or IL-4. Prolonged, 7-day treatment increased autophagosome formation and degradation, while brief activation had no effect. Under parallel culture conditions, IL-13 and IL-4 increased intracellular superoxide levels as determined by electron paramagnetic resonance (EPR) spectroscopy. Prolonged IL-13 activation increased DUOX1, localized at the apical membrane. Silencing DUOX1 by siRNA attenuated IL-13-mediated increases in superoxide, but did not reduce autophagy activities. Notably, depletion of autophagy regulatory protein ATG5 significantly reduced superoxide without diminishing total DUOX1 levels. Depletion of ATG5, however, diminished DUOX1 localization at the apical membrane. The findings suggest non-canonical autophagy activity regulates DUOX1-dependent localization required for intracellular superoxide production during Th2 inflammation. Thus, in chronic Th2 inflammatory airway disease, autophagy proteins may be responsible for persistent intracellular superoxide production.

1. Introduction

Autophagy is a highly conserved process that classically regulates the degradation and recycling of cellular proteins and membranes. The autophagy pathway is triggered in response to changes in metabolic demands of the cell, infection, ER stress, and other cellular stresses including oxidant stress. In lung disease, autophagy may be triggered in response to external cellular stresses such as hypoxia [1,2], endotoxin [3,4], cigarette smoke, and respiratory viral infection, which are all also associated with increased oxidant levels [5–8]. While autophagy occurs

Abbreviations: ALI, Air liquid interface; BSA, Bovine serum albumen; CMH, 1-hydroxy-3-methoxycarbonyl-2,2,5,5-tetramethylpyrrolidine; CM-H2DCFDA, chloromethyl-2′,7′-dichlorodihydrofluorescein; DUOX1, Dual oxidase 1; EPR, Electron Paramagnetic Resonance; EGF, Epidermal Growth Factor; hTEC, human tracheobronchial epithelial cells; IL-13, Interleukin 13; IL-4, Interleukin 4; IL-33, Interleukin 33; NADPH, Nicotinamide adenosine, dinucleotide phosphate; PBS, Ovalbumin (OVA) phosphate buffered saline; PVDF, polyvinylidene fluoride; ROS, reactive oxygen species; SOD, superoxide dismutase

* Correspondence to: Pulmonary Critical Care, Sleep, & Allergy Division, University of Nebraska Medical Center, 985910 Nebraska Medical Center, Omaha, NE 68198-5910, USA.
E-mail address: jdickins@unmc.edu (J.D. Dickinson).
[1] Co-senior authors.

http://dx.doi.org/10.1016/j.redox.2017.09.013
Received 9 June 2017; Received in revised form 8 September 2017; Accepted 18 September 2017
Available online 22 September 2017

in a homeostatic response to these acute insults, persistent elevated autophagy protein levels have been associated with lung diseases. In these high activation states, autophagy regulatory proteins may also participate in so called non-canonical autophagy fates. In these circumstances autophagy proteins can regulate autophagosomes to non-proteolytic pathways or regulate protein secretory machinery [9–13]. Autophagy has been associated with pathologic responses in chronic lung disease, but specific autophagy activities in the oxidant injury responses are unknown.

A current paradigm positions ROS upstream of autophagy activation in response to cell stress [14–20]. In contrast, we previously observed an autophagy-dependent increase in IL-13-mediated total oxidant levels in human airway epithelial cells [21]. However, the source and type of oxidant stress, the conditions contributing to autophagy-dependent ROS generation, and the role of autophagy machinery are unresolved. It has been proposed that autophagy controls ROS generation as a result of regulating NADPH oxidase [12]. In the gut epithelium, the autophagosome is utilized for trafficking NADPH oxidase NOX2 activity through a non-proteolytic autophagosome fate. These findings are consistent with the accumulating data that autophagy proteins have a dual function to direct protein recycling in the lysosome and also to regulate protein secretion and trafficking during stress conditions [9,22].

Th2 cytokines IL-13 and IL-4 function as drivers of chronic inflammation, mucous, cell metaplasia, and oxidant stress in the airway epithelia in asthma and other airway diseases [23–27]. The contribution of the airway epithelial cell to redox balance has been highlighted in reports of increased DUOX1 activity in asthma. DUOX1 is a calcium-activated transmembrane protein member of the NOX family of NADPH oxidases principally located on the apical surface of airway and thyroid epithelia [28,29]. DUOX1 activator protein (DUOXA1) is required for proper maturation and transport out of the ER [30,31]. Previous work found DUOX1 to be a strong generator of hydrogen peroxide (H_2O_2), *via* intra-molecular dismutation of superoxide [32]. DUOX1 is postulated to enhance anti-microbial defense by apical ROS release [33–35]. DUOX1 may also contribute to airway disease pathogenesis. Brief activation with IL-13 has been shown to increase DUOX1 expression and apical hydrogen peroxide levels in culture human airway epithelial cells [36] and human keratinocytes [37]. Furthermore, DUOX1 activity amplifies EGF receptor signaling in Th2 airway inflammatory diseases [38,39]. DUOX 1 knockout mice have reduced IL-33 release, epithelial EGF receptor signaling, and mucous cell metaplasia [39,40], strongly suggesting that DUOX1 participates in the inflammatory signaling cascade in the airway epithelial cell. The factors that direct DUOX1 activity and apical localization are less well established.

We hypothesized that autophagy activity is essential for intracellular superoxide production by regulating NADPH oxidase in airway epithelial cells. Here, we show that persistent IL-13 activation increased superoxide levels in a DUOX1- and autophagy-dependent fashion. Chronic IL-13 increased autophagosome formation, without significantly degrading DUOX1 by means of the autophagosome-lysosome pathway. Depletion of DUOX1 did not affect autophagy activity but depletion of autophagy reduced the IL-13-mediated increase in superoxide levels and impaired proper apical localization of DUOX1.

2. Materials and methods

2.1. Mouse studies

The University of Nebraska Medical Center Institutional Animal Care and Use Committee approved all animal studies. Ten-week-old BALB/c mice (Charles River Laboratories, Willmington, MA), were acclimated for 1 week prior to experimental procedures. Ovalbumin (OVA) sensitization was carried out by intraperitoneal injection of chicken ovalbumin (Grade V; Sigma-Aldrich; A5503) adsorbed with aluminum hydroxide, OVA, 500 μg/mL OVA; alum, 20 mg/mL; injection volume, 100 μL) on days 0, 4, and 7. On days 17, 18, 19, 20, 21, and 24 airway challenge with saline alone or 1.5% OVA in saline was performed in a whole body ultrasonic nebulization plexiglass chamber (DeVilbiss). On day 25, mice were anesthetized with isoflurane and euthanized. The right heart ventricle was injected with a solution of sterile heparin in phosphate buffered saline (PBS) to remove blood from the lung vasculature. Lungs were then resected, formalin fixed and paraffin embedded for immunohistochemistry or processed for mRNA and protein measurements. Freshly excised lung tissue was weighed and homogenized in PBS. Homogenates were cleared of cellular debris by centrifugation at 10,000*g* for 10 min. Mouse IL-4 and IL-13 were measured in homogenates using commercial ELISA kits (Affymetrix; #88-7044-22).

2.2. Cell culture

Human tracheobronchial epithelial cells (hTEC) derived from excess tissue of lungs donated for transplant were cultured on supported membranes (Transwell, 6.5 or 12 mm diameter, 0.4 μm polyester; Corning, #3470) using proliferation medium [41] supplemented with 10 μM Y27632 [42] (Sigma-Aldrich; #Y0503). When cells were confluent they were treated with human recombinant IL-13 (10 ng/mL) or IL-4 (10 ng/mL) (Peprotec; #200-13 or #200-04, respectively) and cultured using air-liquid interface (ALI) conditions with differentiation medium (Pneumocult, Stem Cell Technology; #05001) or Ham's F-12/DMEM supplemented with 2% NuSerum (Corning; #355100) and retinoic acid as described [21,41]. hTEC derived from 12 different donors were used and each experiment used cells derived from at least three donors unless specified otherwise. To detect DUOX1 localization in non-polarized airway epithelial cells, hTEC were seeded directly on collagen-coated glass cover slips and submerged in proliferation medium with IL-13 (10 ng/mL) for 7 days. hTEC were then washed in cold PBS and fixed for 10 min with 4% paraformaldehyde (Affymetrix; #J19943) followed by three washes in PBS.

2.3. Immunostaining

Paraffin wax was removed from mouse lung tissue or hTEC ALI paraffin-embedded sections by incubation with xylene, followed by hydration in three rinses of isopropyl alcohol for 5 min each. Antigen retrieval was accomplished by boiling tissues in Trilogy solution (Cell Marque; 920P-09) for 20 min. Non-specific binding was blocked in 5% donkey serum in 0.1% Triton ×100. Lectin-UEA1 (Vector Laboratories; #RL 1062) was used to identify mucous cells in mouse lung sections. The mouse monoclonal antibody (Thermo Scientific; #MA1-38223) against MUC5AC 45M1 epitope was used in hTEC sections to mark MUC5AC staining. The rabbit polyclonal LC3B (microtubule-associated proteins 1A/1B light chain 3B) antibody (Sigma-Aldrich; #L7543) was used to immunostain autophagosomes in both mouse lung sections and hTEC ALI sections. A mouse monoclonal LC3B antibody (Enzo ALX; 803-080-C100) was used to immunostain LC3B in hTEC when used in combination with anti-DUOX1. A rabbit polyclonal antibody was used for DUOX1 [28] immunostaining. Fluorophore-labeled donkey secondary, species-specific antibodies were Alexa Fluor 488 or 555 (Life Technologies; #A-31570, #A21202, #A21206, #A31572). To localize DUOX1 on hTEC cultured on glass cover slips, fixed cells were blocked with 5% donkey serum in 0.1% Triton ×100 in PBS for 1 h at room temperature. Anti-DUOX1 antibody (1:500) was incubated with cells overnight at 4 °C. After three PBS washes, cells were incubated with fluorescent labeled donkey anti-rabbit secondary antibody and phalloidin (Thermo Fischer; #A12379) conjugated to Alexa 488 nm fluorophore to identify filamentous actin. Cells were incubated for 30 min at room temperature and then washed again with PBS.

2.4. Microscopy and confocal microscopy

Immunofluorescent images were captured using a Zeiss Axio Observer Z.1 microscope and analyzed by Zen software (Zeiss). LC3 puncta from mouse airways were quantified with a common signal threshold using ImageJ (v2.0) as previously described [21]. A Zeiss 710 confocal microscope was used to detect DUOX1 in hTEC with Zen software for image analysis. Co-localization of DUOX1 with phalloidin in 1.5 μm z-stack images was performed using ImageJ (version 2.0) z-stack images were loaded into ImageJ as a sequence, color channels were separated, and the blue channel was discarded. Scatter plots were then generated from each sequence to measure co-localization of red (DUOX1) and green (phalloidin) channels. Signal thresholds of pixel intensity were generated by the Costes method [43]. Pearson coefficients (R) were then measured from each scatter blot to quantify co-localization of green and red signal pixels above the individually calculated signal threshold.

2.5. LC3B flux assay

In vitro autophagy activity was determined by the flux assay for LC3B using chloroquine (50 μM) for transient autophagosome-lysosome disruption as previously described [21,44]. LC3B II and I forms were distinguished by relative molecular weight after separating proteins on a 15% agarose gel. Cells were washed with cold PBS and lysed using RIPA buffer (Sigma-Aldrich; #R0278) containing protease inhibitors (Sigma-Aldrich; #P8340). Protein-containing supernatants were isolated by centrifugation, denatured at 100 °C for 5 min, then briefly disrupted using a water bath sonicator (Branson 5510 model) in four 30-second bursts, and mixed with Laemmli buffer containing 2-mercaptoethanol. Autophagy marker LC3B II levels were assayed by immunoblot using LC3B antibody (1:750 dilution; Sigma-Aldrich; #L7543) on 0.45 μm polyvinylidene fluoride (PVDF) membranes (Immobolin FL; Sigma-Aldrich; IPFL00010). Horseradish peroxidase conjugated goat anti- mouse or rabbit antibodies, respectively, were then used to image primary antibodies with densitometry values normalized to actin. To determine the relevance of STAT6 signaling in autophagy induction, hTEC were lysed in buffer containing NP-40 detergent (0.5%) with 50 mM HEPES (pH 7.0), 5 mM EDTA, 50 mM NaCl, 10 mM Na Pyrophosphate, 50 mM Na fluoride, protease inhibitors (Roche, #11697498001), 100 μM sodium orthovanadate, and freshly prepared phenylmethanesulfonylfluoride (1 mM) dissolved in 200 proof isopropanol. Lysates were centrifuged at 9800*g* 4 °C. Supernatants were then collected and run on 6–15% gradient acrylamide gel and transferred on PVDF membranes. Proteins were blocked in 5% bovine serum albumin for 1 h and then incubated with primary antibodies to STAT6 (1:500 dilution; Cell Signaling; #D3H4) or phosphorylated STAT6 (Tyr641; 1:500 dilution; Cell Signaling; #C11A12) overnight at 4 °C. STAT6 proteins were detected by chemiluminescence as described above.

2.6. Gene expression

RNA was isolated using the RNA Plus Easy kit (Qiagen #74.34) and reverse transcribed (Applied Biosystems; #4308228). DUOX1/2, NOX4, LC3, and MUC5AC transcripts were measured by qRT-PCR with SYBR Green (Qiagen; 330511) using primers listed in Supplement Table 1. Gene expression was reported as fold change over baseline condition normalized to GAPDH in mouse lung tissues and OAZ1 in human cells calculated using the double delta CT ($2^{\Delta\Delta CT}$) method [30].

2.7. RNA interference

ATG5, DUOX1, or control, non-targeted (NT) siRNA sequences (Dharmacon; #L-004374-00-0005, L-008126-00-0005 and #D-00-1810-10–20) are listed in Supplemental Table 1. siRNA sequences were transfected in hTEC on day 0 of culture. The siRNA oligonucleotides (80 nM) were suspended in Opti-MEM 1 (25%; Life Technologies, #31985-070) and Lipofectamine RNAiMAX (Invitrogen; #13778-150), then added to cells in hTEC proliferation media [41]. After 48 h, transfection media was removed and cells were maintained in proliferation medium until the ALI was established. Depletion of ATG5 and DUOX1 was verified on ALI 14 d cells by immunoblot analysis using antibodies to ATG5 (1:1000 dilution; Sigma-Aldrich; #A0856) or DUOX1 (1:500 dilution), respectively. hTEC were solubilized for DUOX1 immunoblot in Laemmli buffer, sonicated then passed through a 27-gauge needle. After denaturing proteins at 95 °C for 5 min, cell lysates were separate by PAGE electrophoresis and transferred to nitrocellulose membranes for DUOX1 or PVDF membranes for actin detection. Membranes were blocked with 5% powdered milk in Tris buffered saline and then incubated with a DUOX1 rabbit antibody or 1:2000 mouse actin antibody. hTEC lysates for ATG5 detection were separate on PAGE in a similar fashion as LC3B and normalized with actin signal. Horseradish peroxidase conjugated to species-specific secondary antibodies were then used to image primary antibodies by chemiluminescence.

2.8. ROS detection

After OVA or saline airway challenge, lungs were excised, and injected intratracheally with dissociation solution containing dispase II (Sigma-Aldrich; #D4693-1G), 10 units diluted in 1.2 mL of Hank's modified saline solution. The cell solution was sequentially passed through a 22-gauge needle and 20-micron filter. To detect ROS, cells were incubated in the oxidant sensitive fluorometric probe DCF (5 μM; CM-H2DCFDA; Life Technologies; #C6827), dissolved in HBSS for 8 min. Next DCF labeled cells were washed in HBSS and then incubated with an antibody to the pan-epithelial cell marker CD326 (BioLegend; #118211). Cells were washed again prior to isolation of $CD326^+$; DCF^+ and $CD326^+$; DCF^- cell populations using flow activated cell sorting (Bectin-Dickinson LSR II Flow Cytometer with BD FACSDIVA Software).

Superoxide-specific levels were measured *in vitro* using the cell permeable superoxide-sensitive electron paramagnetic resonance (EPR) spectroscopy spin probe, 1-hydroxy-3-methoxycarbonyl-2,2,5,5-tetramethylpyrrolidine (CMH), 200 μM as previously described [45,46]. hTECs cultured using ALI conditions were incubated with 200 μM CMH in KDD buffer consisting of Krebs-HEPES containing deferoxamine mesylate salt (25 μM) and diethyldithiocarbamic acid sodium salt (DETC, 5 μM). The CMH spin probe in KDD [45] buffer was added to the basal compartment of the Transwell for 30 min at 37 °C. Cells were then scraped from the apical surface of the membrane with a pipet tip and suspended in KDD buffer plus CMH from the basal chamber. Superoxide levels were then immediately measured using a Bruker e-scan EPR spectrometer. The amplitude of the EPR spectrum was normalized to total cellular protein taken from each cell sample. To assess the role of hydrogen peroxide as an intermediary for superoxide, we next treated hTEC with IL-13 and IL-4 (10 ng/mL) and added apical catalase 800 Units (Sigma-Aldrich; #C1345) in 20-microliter volume of PBS at day 1,3,5, and 7. EPR spectroscopy to measure intracellular superoxide was performed on day 7.

Extracellular hydrogen peroxide was measured by Amplex Red assay (Invitrogen; #A22188) as previously described [28]. In brief, warm PBS was added to the apical surface of hTEC for 1 h at 37 °C. Samples were collected and mixed 1:1 ratio with a solution of horseradish peroxidase 10 U/mL and Amplex Red 10 mM. Mixtures were incubated in the dark for 30 min, at room temperature. The fluorescent Ex530/Em590 spectrum was recording using a Spectramax i3x microplate reader (Molecular Devices). Readings were quantified by a standard curve of hydrogen peroxide and corrected for the surface area of cells in ALI hTEC inserts.

2.9. Measurement of superoxide dismutase enzyme activity

Lungs were excised from mice challenged with saline or OVA, and rinsed in ice cold PBS containing protease inhibitors (Sigma-Aldrich; #P8340), then dissociated with cup-horn water sonication for 3–4 ten second bursts or until the lysate was clear. Lysates were then centrifuged at 10,000*g* for 10 min at 4 °C. The cell-free supernatant was collected and analyzed for total SOD enzyme activity and copper/zinc SOD activity (SOD1) using the SOD Assay Kit-WST (DOJINDO; #S311-10) per the manufacturer's instructions. Total SOD and SOD1 activity was normalized to total protein in the lung homogenate. SOD1 protein levels were measured by immunoblot of lung homogenates after water bath sonication, separated on 6–15% gradient polyacrylamide gel, and transferred to PVDF 0.45 μm membranes for 2 h. Protein was detected with rabbit polyclonal SOD1 specific antibody (Santa Cruz; #SC-11407). Protein bands were detected with chemiluminescence as described above and levels normalized to actin. To detect LC3B levels in lungs from OVA or saline challenged mice, freshly excised lungs were homogenized in RIPA buffer with protease inhibitors and disrupted using a steel bead mill. Lung lysates were then centrifuged at 9800*g* for 10 min at 4 °C. Supernatants were collected and prepared for LC3B immunoblots as described above.

3. Results

3.1. OVA-induced inflammation increases autophagy activity and ROS levels

To evaluate autophagy activity, we used an allergen-driven airway disease model that results in a dominant Th2 inflammatory response. The airways of BALB/c mice were challenged with aerosolized OVA after intraperitoneal sensitization (Fig. 1**A**). The Th2 cytokines, IL-13 and IL-4 were increased in lung tissue obtained one day after the final airway OVA exposure (Fig. 1**B,C**). Th2 inflammation in the airways was associated with an increase in mucous cell metaplasia as noted by immunohistochemistry (Fig. 1**D**) and overexpression of the inflammatory mucin, MUC5AC (Fig. 1**E**). Having previously shown a relationship between IL-13 and autophagy induction *in vitro* [21], we examined the levels of autophagy marker in the LC3BII in whole lungs homogenates. Compared to control mice, LC3BII levels were significantly increased in lung tissues from OVA challenged mice indicating increased autophagosome levels (Fig. 1**F,G**). We localized the LC3B puncta to epithelia by immunostaining lung sections from the same mice. Increased numbers of LC3B puncta were present in airway epithelial cells following OVA challenges compared to saline treatment, which had little detectable epithelial cell staining (Fig. 1**H,I**). From these data, we conclude that Th2 inflammation *in vivo* was associated with increased numbers of autophagosomes in airway epithelial cells.

Our prior *in vitro* studies demonstrate a direct relationship between Th2 inflammation, autophagy, and ROS [21]. DUOX1 is up regulated in epithelial cells from asthmatics [39], and in cultured airway epithelial cells within 72 h of *in vitro* activation by IL-13 and IL-4 [36]. We found a marked increase in DUOX1 expression in the lungs of OVA-treated mice, compared to controls. While there was also a statistically significant increase in DUOX2 expression, the DUOX1 increase was magnitudes higher (~ 70-fold *vs.* 2-fold increase) (Fig. 2A,B). Levels of NOX4, another NADPH oxidase protein reportedly associated with inflamed airway epithelial cells [47], slightly decreased after OVA challenge (Fig. 2**C**). To directly measure oxidant levels in the epithelial cells, we collected airway epithelial cells dissociated from the lungs of OVA- or saline-challenged mice. In the bulk lung cell population isolated from OVA-challenged mice, there was a significant increase in total DCF-positive cells, indicating an increase in total oxidant levels (Fig. 2**D,E**). Increased oxidant levels were specifically identified in the epithelia by co-staining of DCF with pan-epithelial marker CD326 (Fig. 2**F,G**). Activity of SOD1, which converts superoxide to hydrogen peroxide (H_2O_2), is reduced in airway epithelial cells of asthmatics [48–50]. As expected, ROS was accompanied by changes in SOD activity in the OVA-challenged model. There was a decrease in SOD1 activity and SOD1 protein levels in OVA-challenged mouse lungs (Fig. 2**H–K**) suggesting that the airway epithelium is less protected against superoxide-induced injury. Taken together, our observations demonstrate that autophagy is elevated in airway epithelial cells during *in vivo* Th2-mediated inflammation, accompanied by increased DUOX1 expression and elevation in ROS levels.

3.2. Autophagy requires prolonged Th2 cytokine stimulation in airway epithelial cells

To more specifically examine the role of autophagy in the production of Th2-induced superoxide in airway epithelium, we utilized primary-culture human tracheobronchial epithelial cells (hTEC). Autophagy activity was determined by assay of LC3 turnover using chloroquine treatment followed by measurement of isoform LC3BII levels ("flux assay") (Fig. 3**A**). LC3B II is the form found exclusively on the autophagosome while LC3B I is found in the cytoplasm. Chloroquine alters the pH of lysosomes to reduce autophagosome-lysosome degradation and eliminate the consumption of autophagy proteins used to form the membranes that surround target proteins and form the autophagosome [44]. We identified Th2 cytokine treatment conditions that activate autophagy in the presence of chloroquine then measured the accumulation of autophagosome bound LC3BII in well-differentiated hTEC. Brief stimulation of autophagy for 3 h (3 h) with mammalian target of rapamycin (mTOR) inhibitor, Torin1, increased LC3BII levels by immunoblot. There was both an increase in autophagosome levels (dashed line over bars) and autophagy flux activity with increased LC3B degradation in the lysosome (solid line over bars) (Supplemental Fig. 1**A,B**). In contrast, after three hours, there was a non-cytokine specific increase LC3BII in the presence of chloroquine (Supplemental Fig. 1**C–F**). The lack of cytokine specific autophagy activity occurred despite IL-13 and IL-4 signaling as indicated by the expected [51] increase in phospho-STAT6 levels (Supplemental Fig. 1**G,H**). We interpreted these data to indicate that cytokine-induced up regulation of autophagy does not rely on immediate signaling through the known IL-13/-4 receptor heterodimer.

Inflammatory airway diseases such as asthma are associated with repeated and chronic activation by Th2 cytokines [52]. Prolonged activation with IL-13 or IL-4 for 7 days (7d), increased LC3BII levels by immunoblot (Fig. 3**B**). The LC3B chloroquine autophagy flux assay was again used to compare autophagosome membrane synthesis with autophagosome-lysosome degradation. hTEC treated with IL-13 or IL-4 plus chloroquine compared to chloroquine alone had a significant increase in LC3BII levels reflecting increased autophagosome synthesis. (Fig. 3**C,D dashed lines**). hTEC treated with cytokine plus chloroquine compared to cytokine alone had a detectable but non-statistically significant increase in LC3BII levels reflecting autophagosome degradation (Fig. 3**C,D solid lines**). The increased autophagosome membrane synthesis without, comparable increase in LC3B autophagosome-lysosome degradation suggests that a fraction of the cytokine-stimulated autophagosomes have a non-degradation fate. One possible explanation for the observed increase in the autophagosomes was that the expression of LC3B was affected by chronic IL-13 or IL-4 activation at the transcriptional level. Yet, there was no significant difference in LC3B mRNA expression between naïve and treated cells (Fig. 3**E**). We next tested if the IL-13 or IL-4-induced increase in autophagosomes was sustained after withdrawal of the cytokine. Autophagy activity remained elevated after a 5-day washout period without cytokine (Fig. 3**F**). These findings indicate that prolonged activation with Th2 cytokines increased and sustained autophagosome and autophagy protein levels in well-differentiated airway epithelial cells.

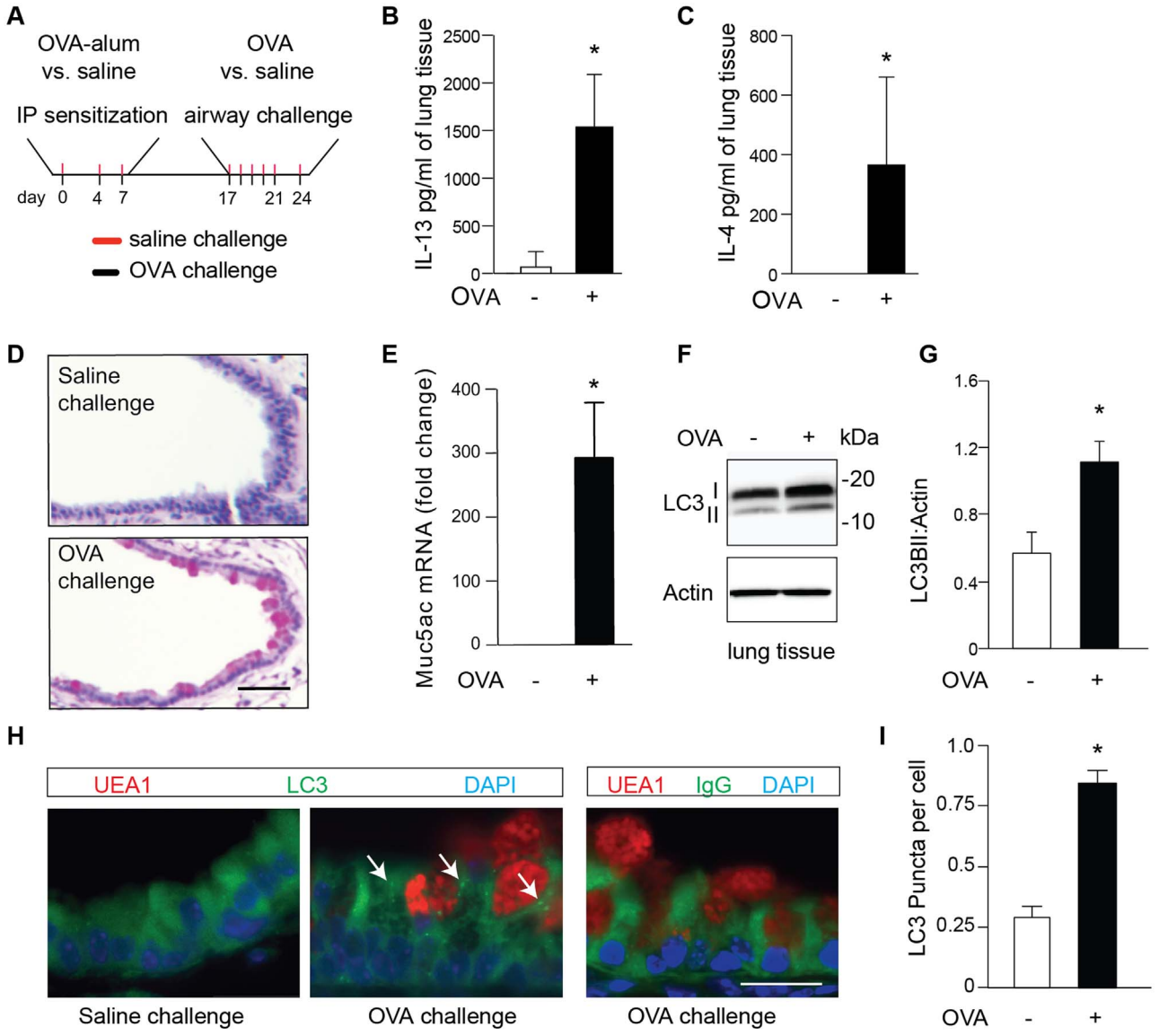

Fig. 1. *OVA-challenge increased Th2 cytokines and autophagy in airway epithelial cells.* (A) Schematic for BALB/c mice challenged with nebulized airway OVA or saline after sensitization. Th2 cytokines IL-13 (B) and IL-4 (C) were quantified in lung homogenates by ELISA (n = 6 mice per group). (D) Airways from lungs of saline (-) or OVA (+) challenged mice were sectioned and stained for mucus cells by PAS. Scale bars = 50 μm. (E) MUC5AC was measured by qPCR from lung homogenate (n = 6 mice per group). LC3B levels in lungs from saline (-) and OVA (+) challenged mice were analyzed by immunoblotting (F). (G) LC3B II was normalized to actin (n = 8 mice per group). (H) Representative images of LC3B (green puncta) and mucin marker lectin-UEA1 (red) in airway epithelial cells from lungs of OVA or saline challenged mice detected by immunostaining. White arrows indicate LC3B puncta. IgG isotype controls are provided for puncta staining. (I) Puncta number were normalized to 4′,6-diamidino-2-phenylindole (DAPI) positive cells in airway epithelia. Six, high-magnification images from lung tissues of 4 mice from each condition were quantified for LC3B puncta in airway epithelial cells and normalized to the total number of cells identified by nuclear DAPI. Scale bar = 20 μm. Shown is the mean ± SEM in each condition. A significant difference between groups was determined by the unpaired *t*-test (*, $p < 0.05$).

3.3. IL-13 and IL-4 increase intracellular superoxide levels

Previous work identified that Th2 cytokines increased apical hydrogen peroxide levels in primary human airway epithelial cells [36]. Our data (Fig. 2**H–K**) confirms the findings others have reported regarding loss of SOD1 activity in asthma and asthma models [48–50,53]. Considering SOD1 scavenges intracellular superoxide, this focused our attention on superoxide levels, which have not been previously characterized in airway epithelial cells during Th2 inflammation. To address the role of Th2 cytokine-induced superoxide, we measured intracellular superoxide levels using the superoxide-sensitive spin probe, CMH [54], and EPR spectroscopy. We used the same brief (3 h; 3 h) and the prolonged (7 day; 7 d) Th2 cytokine activation protocols used to assess autophagy (Fig. 4**A**). At 3 h, IL-4 slightly decreased superoxide levels and IL-13 treatment had no effect (Fig. 4**B,C**). In contrast, yet consistent with the observed temporal activation of autophagy, prolonged treatment (7 d) with IL-13 or IL-4 significantly increased intracellular superoxide levels (Fig. 4**D–F**). The intracellular superoxide persisted as long as 5 days after inflammatory cytokines have been withdrawn (Fig. 4**G,H**), confirming that airway epithelial cells are significant sources of intracellular superoxide during and after Th2 cytokine stimulation. These findings parallel the increased autophagy activity observed after a 5-day cytokine washout period (Fig. 3**F**). Similar to the superoxide findings, we found that longer stimulation, for 7 days with IL-13 plus IL-4 was required to stimulate apical hydrogen peroxide levels (Fig. 4I). The addition of catalase to the apical cell surface of hTEC on days 1,3,5, and 7 suppressed extracellular hydrogen peroxide (Supplemental Fig. 2), however, failed to reduce the 7-day cytokine-stimulated increase in intracellular superoxide (Fig. 4**J**).

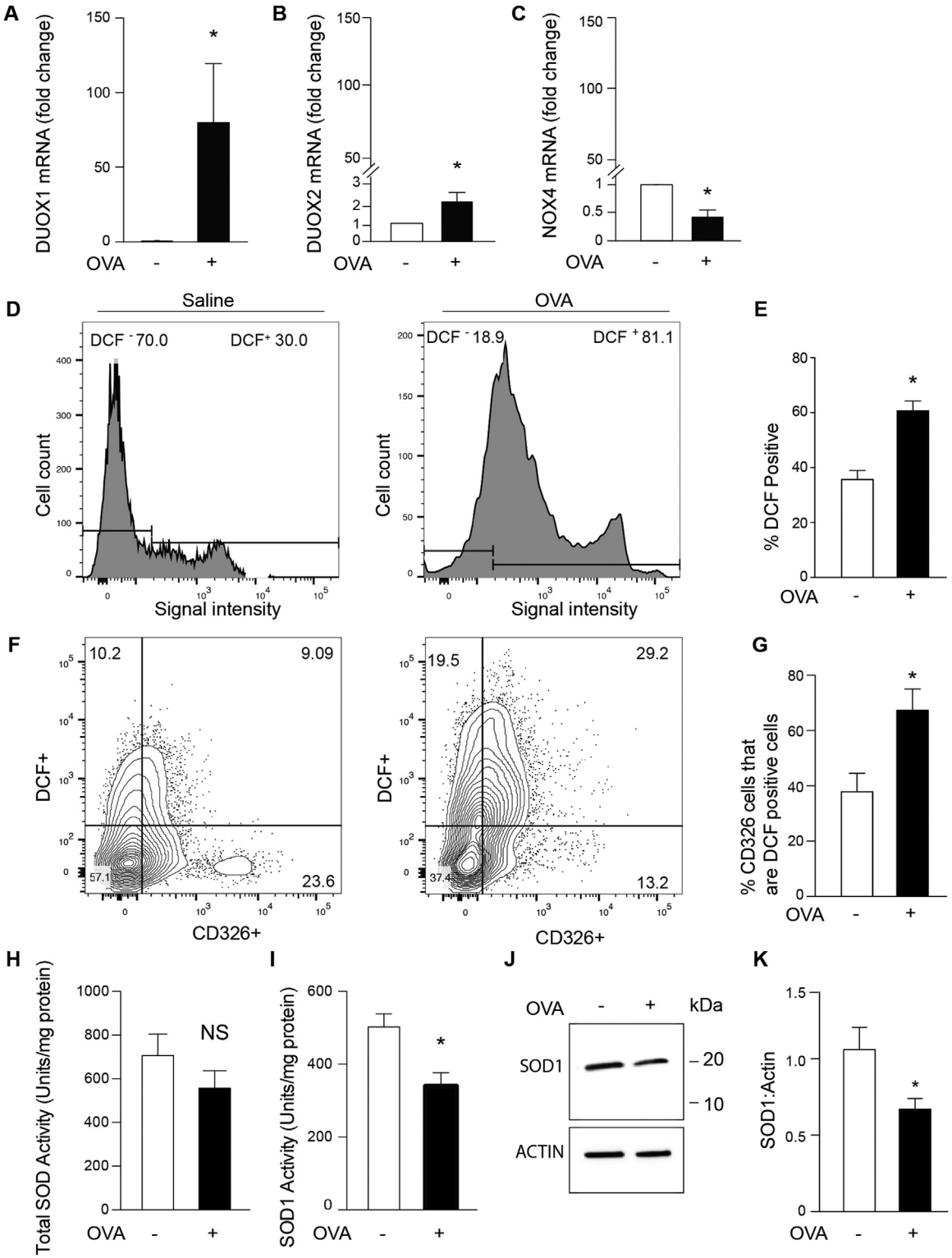

Fig. 2. *Increased DUOX1 and ROS in lungs of OVA challenged mice.* (A) DUOX1, (B) DUOX2, and (C) NOX4 expression was measured in lungs of OVA (+) or saline (-) challenged mice by qPCR (n = 7 mice per group). (D) ROS in isolated lung cells from mice challenged with either saline or OVA detected with oxidant sensitive fluorometric probe, DCF. Representative flow cytometry plots from saline and OVA challenged mice are shown for DCF^+ signal (upper panels) *vs.* (F) DCF^+CD326^+ labeling (lower panels). (E) Quantification of percent DCF^+ out of total cell fractions from panel D (n = 11 mice). (G) Quantification of percent $CD326^+$ cells that are DCF^+ in OVA (+) or saline (-) challenged mice from panel F (n = 11 mice). (H, I) Superoxide dismutase (SOD total and SOD1 specific) enzyme activity (units/mg protein) in mouse lungs challenged with saline or OVA (n = 7). (J) Representative SOD1 protein immunoblot with quantification (K) from lung lysates after measuring SOD1 enzyme activity in mice challenged with saline or OVA (n = 7). Shown is the mean ± SEM in each condition. A significant difference between groups was determined by paired *t*-test (A–C) or unpaired *t*-test (E, G–K), (*, $p < 0.05$).

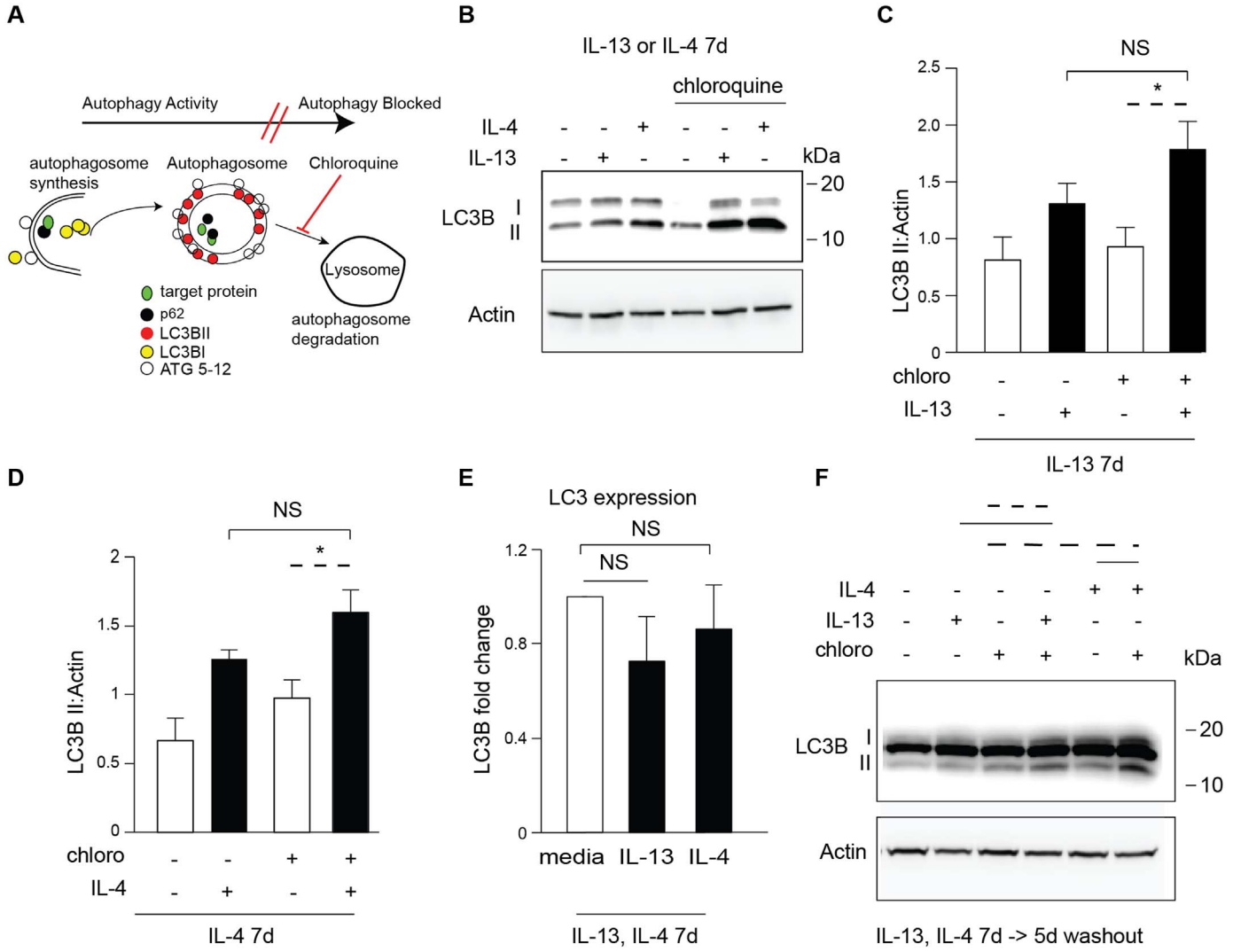

Fig. 3. *Prolonged stimulation with IL-13 and IL-4 increases autophagy in airway epithelial cell cultures (hTEC).* (A) Schematic for autophagosome synthesis and lysosomal degradation using the autophagy chloroquine flux assay. (B) Autophagy activity in well-differentiated (ALI 21 days) hTEC treated with IL-13 or IL-4 (10 ng/mL each) for 7 days (d). Autophagy was detected by flux assay using chloroquine (chloro) inhibition and LC3B immunoblot analysis. (C, D) Quantification of LC3B II band densitometry relative to Actin was performed from (A, B) for IL-13 (n = 5) and IL-4 (n = 4). (E) LC3B gene expression measured by qPCR in hTEC treated with IL-13 (n = 5) or IL-4 (n = 4), both using 10 ng/mL for 7 days. (F) Autophagy in hTEC treated with IL-13 or IL-4 for 7 days followed by a 5 day washout period in standard media prior to measurement of LC3B flux assay. A significant difference between groups was determined by ANOVA with significant Tukey's post-hoc comparison (*, $p < 0.05$; NS = not significant). Solid lines over bars denote change in autophagy flux; dash lines over bars denote changes in autophagosome synthesis.

3.4. DUOX1 is required for chronic IL-13 induced superoxide production, but not autophagy

We next sought to identify the role of DUOX1 relative to autophagy during IL-13 activation. hTEC cultured at ALI treated with IL-13 for 7 d modestly increased levels of DUOX1 mRNA (Fig. 5**A**). As expected, IL-13 activation increased DUOX1 protein along the apical membrane of differentiated epithelial cells, detected by immunofluorescent staining (Fig. 5**B**). Autophagy marker, LC3B, however did not co-localize with DUOX1 at the apical membrane, instead was present diffusely within the cytoplasm (Fig. 5**C;** Supplemental Fig. 3). This finding supports the hypothesis that DUOX1 was not being degraded as a target of autophagy. We then sought to examine the effect of reducing DUOX1 in hTEC using siRNA (Fig. 5**D**). Depletion of DUOX1 abrogated the IL-13-mediated increase in superoxide levels as measured by EPR (Fig. 5**E**). Knockdown of DUOX1, however, did not affect IL-13-mediated increase in autophagosome synthesis, as determined by the autophagy flux assay with LC3B immunoblotting (Fig. 5**F,G**). In agreement with our previous findings suggesting a role for autophagy with MUC5AC secretion [21], IL-13 increased LC3 puncta staining surrounding MUC5AC+ cells in both control and DUOX1 knockdown cells (Fig. 5**H;** Supplemental Fig. 4). These findings suggest that DUOX1 is critical for IL-13-mediated cellular superoxide production in airway epithelial cells and operates downstream of proteins activated for autophagy.

3.5. The cytokine-mediated increase in superoxide is autophagy dependent

The parallel induction of both autophagy and superoxide production in hTEC under similar conditions led us to propose that these pathways were convergent. To test this, we depleted the autophagy regulatory protein ATG5 by siRNA in hTEC, leading to reduced autophagy compared to non-targeted (NT) siRNA transfected control cells (Fig. 6**A–C**). Following chronic IL13 stimulation (7d), the ATG5-deficient cells failed to increase superoxide levels, as measured by EPR spectroscopy (Fig. 6**D**). However, reduction of ATG5 did not affect the IL-13-induced increase in DUOX1 mRNA or protein levels (Fig. 6**E–G**). This indicated that DUOX1 does not undergo significant proteolytic degradation in the lysosome *via* autophagy activity- suggesting that

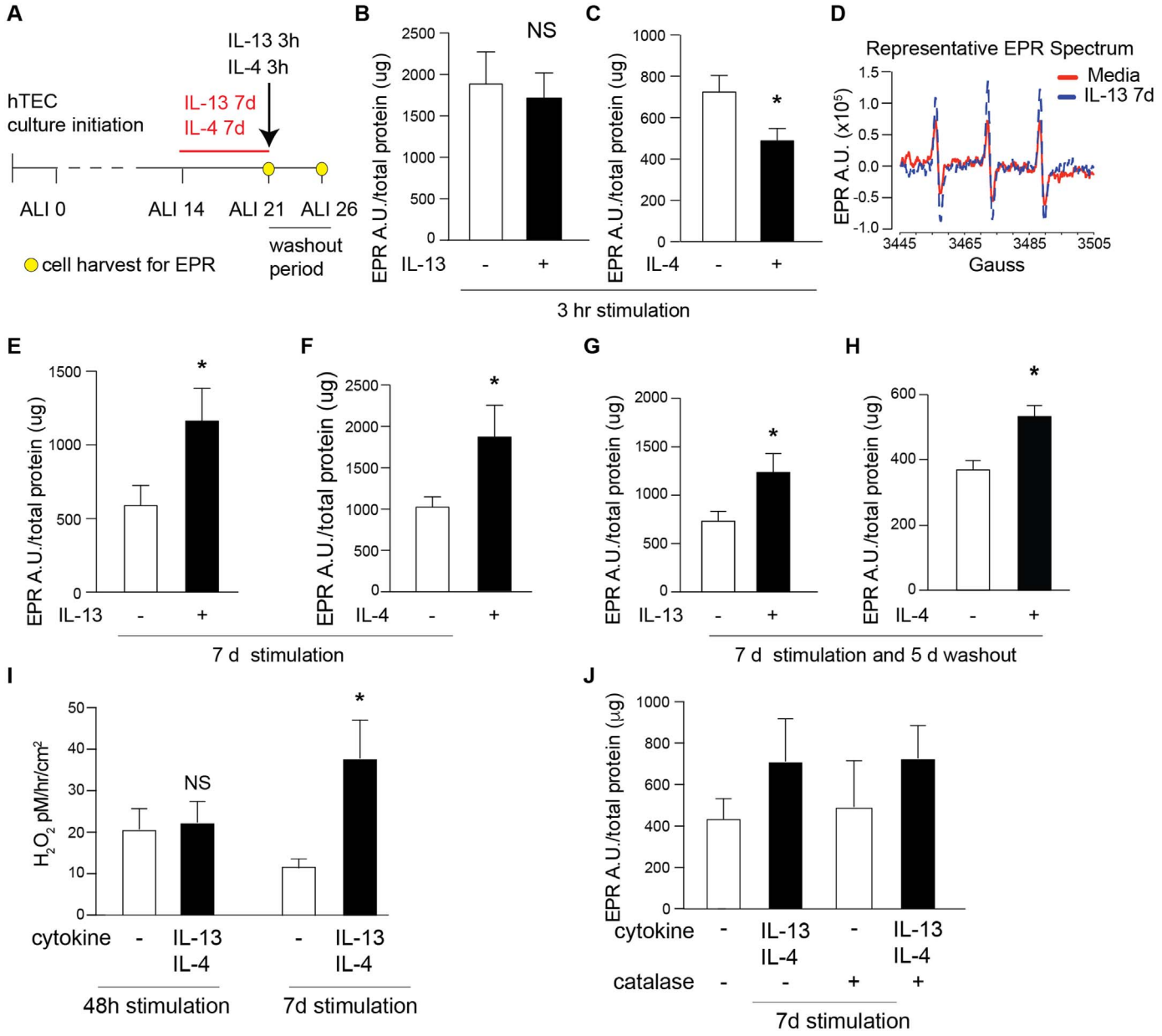

Fig. 4. *Prolonged stimulation with IL-13 and IL-4 increases superoxide levels in airway epithelial cell cultures.* (A) hTEC treatment schematic prior to EPR spectroscopy with CMH spin probe. (B, C) hTEC were treated with IL-13 or IL-4 (100 ng/mL) for 3 h (n = 7 for IL-13 and n = 6 for IL-4). (D) Representative EPR spectra of hTEC treated with IL-13 (10 ng/mL) for 7 days. (E, F) Quantification of EPR data from hTEC treated with IL-13 (10 ng/mL, n = 9) or IL-4 (10 ng/mL, n = 10) for 7 days. (G, H) Quantification of EPR in hTEC treated with IL-13 or IL-4 (10 ng/mL each) for 7 days followed by 5 days washout period in standard media prior to measurement of ROS (n = 6 for both cytokine stimulation experiments). (I) Apical hydrogen peroxide was measured from hTEC by Amplex Red assay treated with basilar IL-13 + IL-4 (10 ng/mL each) for the indicate time periods (n = 7 48hr and n = 8 for 7 d comparison respectively). (J) EPR was performed on hTEC treated with IL- IL-13 + IL-4 for 7 d treated with apical PBS or catalase 800U (n = 3). All EPR levels were normalized to total protein. EPR A.U. is EPR spectra amplitude in arbitrary units. Data are the mean ± SEM in each condition. A significant difference between groups was determined by the unpaired *t*-test (*, $p < 0.05$; NS = not significant).

autophagy functionally regulates superoxide levels, independent of DUOX1 expression or autophagy-mediated degradation. OVA-induced Th2 cytokine inflammation reduced superoxide dismutase (SOD1) levels *in vivo* (Fig. 2**H–K**). There were no change SOD1 levels, however, in autophagy-deficient hTEC stimulated with IL-13 for 7 d (Fig. 6**H,I**). This suggests that autophagy does not regulate superoxide levels *via* SOD1. We therefore considered other factors that may affect DUOX1 functions.

To assess non-canonical autophagosome functions, we next investigated whether the autophagosome regulated DUOX1 localization. Immunostaining of ATG5-deficient hTEC demonstrated reduction of apical DUOX1 localization in hTEC cultured under ALI conditions (Fig. 7**A;** Supplemental Fig. 5). To better quantify DUOX1 localization, undifferentiated, non-polarized hTEC were transfected with ATG5 and NT siRNA were cultured on glass cover slips and treated with IL-13 for 7 d. After treatment, fixed cells were visualized by confocal microscopy. There was significantly reduced DUOX1 localization to the cell cortical membrane, as marked by phalloidin staining for filamentous actin (Fig. 7**B,C**). These findings indicate that autophagy regulates IL-13-mediated increase in superoxide levels by directing DUOX1 to the apical surface of the airway epithelium (Fig. 7**D**).

4. Discussion

Here, we describe how autophagy promotes an increase in intracellular superoxide levels by regulating DUOX1 during Th2 inflammation of the airway epithelium. Our initial observation using the

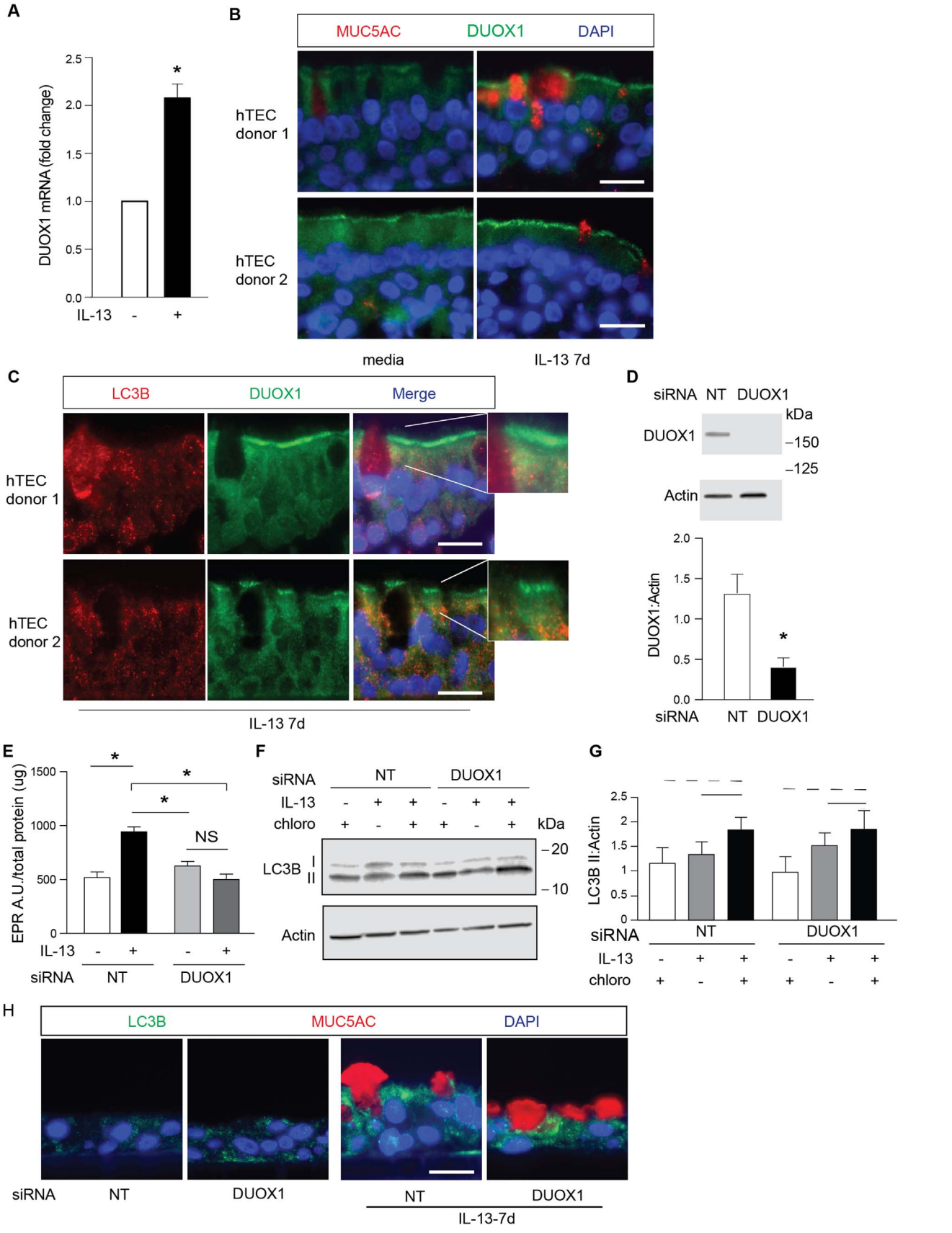

(caption on next page)

Fig. 5. *IL-13 induced superoxide is DUOX1 dependent.* (A) DUOX1 expression measured in hTEC after treatment with IL-13 (10 ng/mL; n = 5) for 7 days. (B) DUOX1 (green) and MUC5AC (red) in well-differentiated hTEC treated ± IL-13 (10 ng/mL) for 7 days, using immunostaining. Shown are representative images from 2 unique hTEC donors. (C) Representative images from two unique hTEC donors of LC3B (red) and DUOX1 (green) immunofluorescent staining after treatment of IL-13 for 7 days. Inset to the right of the merged images is magnified to show cytoplasmic LC3 puncta. Supplemental Fig. 3 presents additional images from same hTEC donors. (D) Representative immunoblot showing DUOX1 levels after transfection with non-targeted (NT) or DUOX1-specific siRNA used for experiments in panels E–H. Quantification from image densitometry for DUOX1 relative to Actin is shown below immunoblot (n = 9). (E) EPR measurements in hTEC transfected with NT or DUOX1 siRNA and treated with IL-13 for 7 days (n = 5). (F) Representative immunoblot with corresponding quantification (G) (n = 4) of LC3 chloroquine flux assay for autophagy activity with and without IL-13 treatment for 7 days. Solid lines over bars denote change in autophagy flux; dash lines over bars denote changes in autophagosome synthesis. (H) Representative images of LC3B puncta staining (green) and MUC5AC staining (red) in NT or DUOX1siRNA hTEC treated with or without IL-13 7 days. Supplemental Fig. 4 shows larger set of images from these cells. Shown is the mean ± SEM in each condition. A significant difference among groups was determined by *t*-test (A) or ANOVA with significant Tukey's post-hoc comparisons (E) (*, p < 0.05; NS = not significant). Scale bar = 20 μm.

oxidant-sensitive fluorogenic probe, DCF, suggested that an autophagy-dependent IL-13-mediated signal was required for secretion of mucin MUC5AC [21]. We have now extended this observation to identify the requirement of the autophagosome for DUOX1-mediated superoxide production. DUOX1 has been identified as a major ROS driver in the airway epithelial cells [39,40,55,56]. We demonstrated the relationship between autophagy and ROS in airway epithelial cells in three approaches: an *in vivo* mouse allergen model, a cytokine activated primary culture system, and following *in vitro* gene silencing. In the setting of OVA-induced inflammation in mice, we found that autophagosome marker LC3B is increased in concert with ROS in the airway epithelial cells by measuring increased production of autophagy protein LC3IIB by immunoblot and immunostaining for LC3B puncta. *In vitro*, primary human airway epithelial cells treated with IL-13 showed increased LC3BII signal, and depleting autophagy protein ATG5 in the same primary culture model showed decreased intracellular superoxide. Unexpectedly, interruption of the autophagy pathway by ATG5 silencing in IL-13 activated cells did not change total DUOX1 levels, but instead,

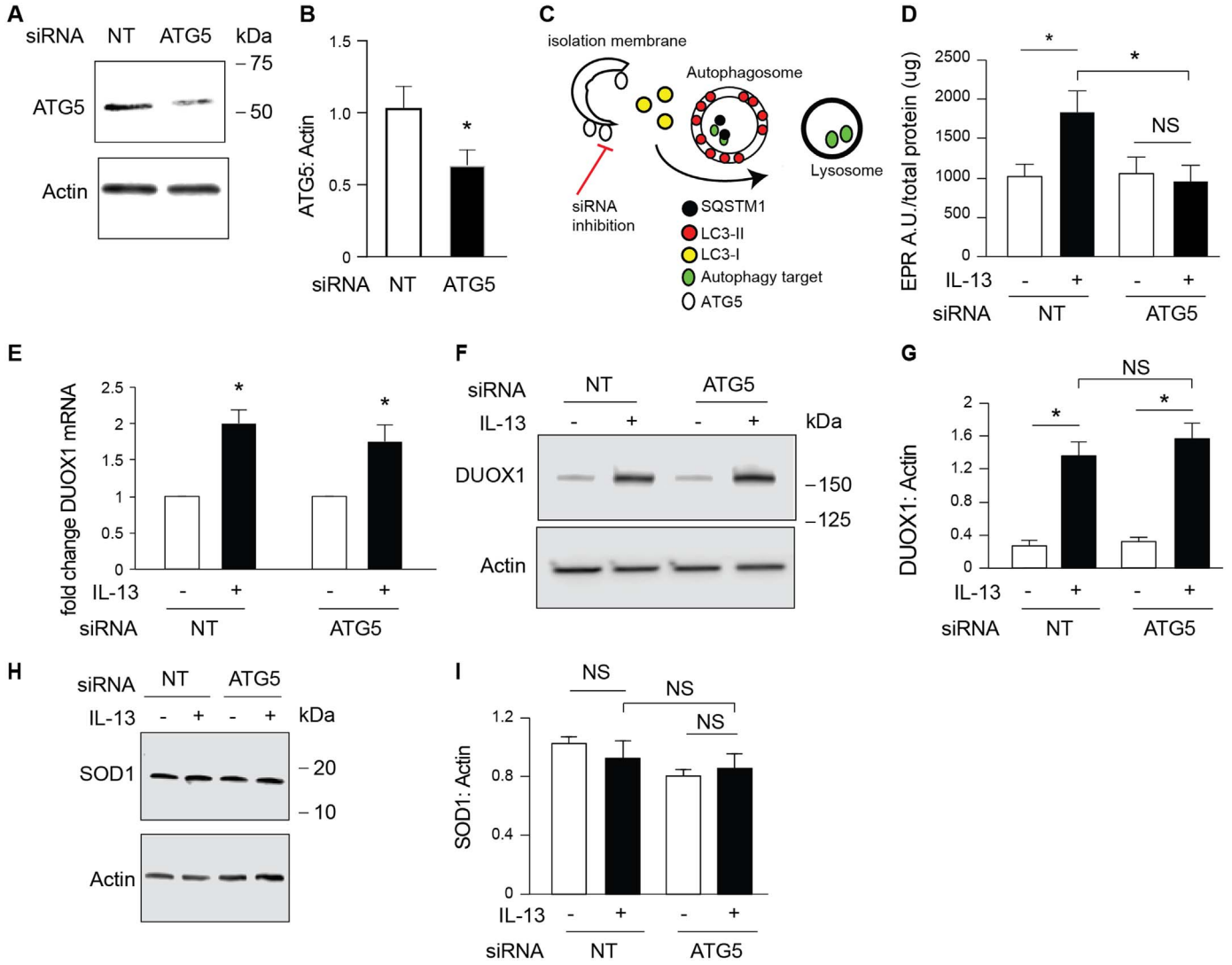

Fig. 6. *Airway epithelial cell cytoplasmic superoxide requires autophagy.* (A) Representative ATG5 immunoblot with quantification from band densitometry for ATG5 relative to Actin from hTEC transfected with ATG5-specific siRNA or non-targeted control sequence (NT). (B) Quantification of ATG5 depletion by western for n = 12 for experiments described in panels D–G. (C) Cartoon depicting depletion of ATG5 leading to reduction of elongation and maturation of autophagosome. (D) Quantification of EPR levels from hTEC transfected with siRNA as in (A) and treated with media (-) or IL-13 for 7 d (n = 7). (E) Fold change of DUOX1 expression with IL-13 for 7 days activation in NT and ATG5 siRNA transfected hTEC measured by qPCR (n = 6). (F) Representative immunoblots of DUOX1 protein levels in ATG5 deficient hTEC treated with and without IL-13 for 7 days and corresponding quantification in (G) (n = 3). (H) Representative immunoblot of SOD1 levels by western blot in hTEC transfected with siRNA as above with corresponding quantification (I) (n = 5). A significant difference between groups is denoted by ANOVA with Tukey's post-hoc comparison (D,G,I) or paired *t*-test for mRNA fold change in (A,E) (*, p < 0.05; NS = not significant).

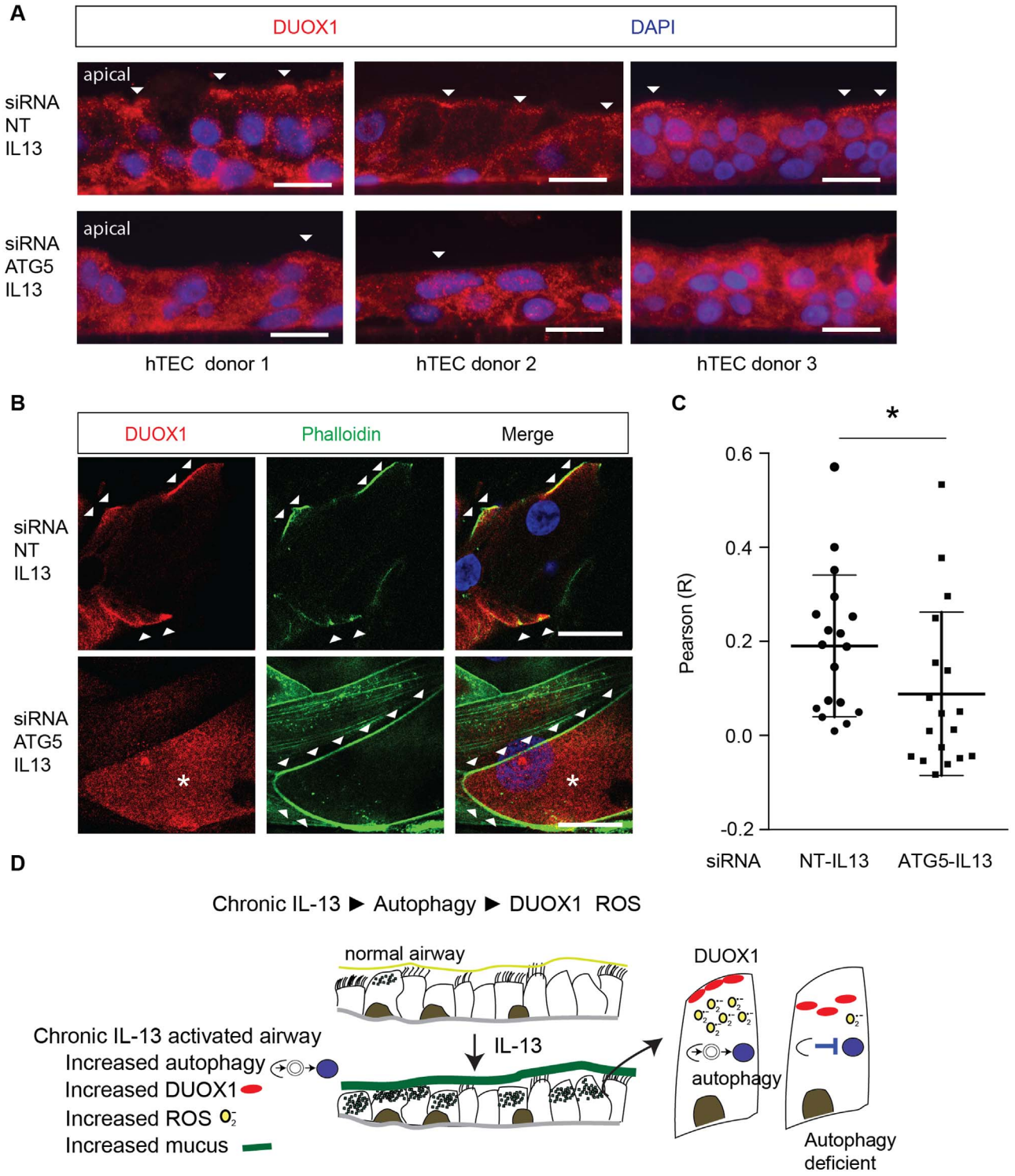

Fig. 7. *Autophagy regulates DUOX1 localization.* (A) Representative images of DUOX1 (red) localization in hTEC treated with IL-13 and non-target or ATG5-specific siRNA, cultured under ALI conditions. DAPI (blue) marks nuclei and arrowheads denote the apical surface. Shown are hTEC derived from 3 different donors. Scale bar = 20 μm. See Supplemental Fig. 4 for a larger set of images from these hTEC donors. (B) Representative confocal images of DUOX1 staining with phalloidin marking actin staining of the plasma membrane in undifferentiated, non-polarized cells from NT and ATG5 deficient hTEC on glass cover slips treated with IL-13 for 7d. Scale bar = 25 μm. (C) Quantification of signal co-localization using Pearson coefficient (R values) of red (DUOX1) and green (phalloidin) channels from NT and ATG5 siRNA transfected cells treated with IL-13. N = 3 hTEC donors with 3–5 z-stack confocal image sequences per donor. A significant difference in co-localization between groups was determined by the Mann Whitney *U* test (*, $p < 0.05$). (D) Model of the role autophagy plays in maintaining oxidant signaling in the airway epithelium. Th2 cytokines activate inflammatory pathways in the epithelium including MUC5AC expression and secretion, elevated superoxide levels ($O_2^{\bullet-}$), and autophagy activity. Autophagy is required for localization of functional DUOX1.

blocked the apical membrane localization. These findings suggest that DUOX1 is dependent on autophagy to regulate specific epithelial functions that are activated in chronic Th2 inflammatory airway diseases such as asthma, COPD and cystic fibrosis [8,57–59].

Oxidant stress is a well-recognized activator of autophagy [17,60]. Our finding that autophagy activates ROS is contrary to that paradigm,

suggesting that the relationship between ROS and autophagy is cell context dependent. The current paradigm derives from observations that serum starvation of cancer cells induced autophagy *via* superoxide action on ATG4 [14,16,20] and that superoxide and hydrogen peroxide can activate autophagy, principally in cancer cell lines [61]. In our chronic model relevant to human disease, Th2 cytokine induced autophagy did not require DUOX1-mediated ROS. Instead autophagy activity was required for the increase in intracellular superoxide production.

The IL-13- and IL-4-mediated increase in autophagy was not dependent on immediate STAT6 signal transduction pathways after brief stimulation but rather on changes in epithelial cell function that occur with chronic cytokine stimulation. Our data support the concept that sustained epithelial injury driven by repeated cytokine inflammation requires autophagy. We show that Th2 inflammation induces both increased apical hydrogen peroxide and increased intracellular superoxide levels. We confirm the previous findings that Th2 activation increases apical hydrogen peroxide [40] and broaden the diversity of oxidant signaling by identifying increased intracellular superoxide levels in the airway epithelium. The requirement for chronic stimulation by Th2 cytokines for increased intracellular superoxide suggests a ROS-induced ROS mechanism leading to increased superoxide. Furthermore, epithelial cells exhibit oxidant "memory" by displaying persistently high levels of superoxide after the withdrawal of IL-13 or IL-4, as we demonstrated in an *in vitro* washout model. Clinically, this may be relevant, as Th2-type asthma is driven by repetitive allergen stimulation, which release epithelial-derived IL-33 and cause lymphocytes to secrete Th2 cytokines such as IL-13 and IL-4 [52,62]. Thus despite the periodic nature of airway allergen challenge, persistent oxidant stress may be propelled by epithelial autophagy activity. Future studies will examine the mechanism by which DUOX1 mediates an increase in intracellular superoxide and how autophagy regulates DUOX1 localization and function.

Classically, autophagy is a broad, largely homeostatic pathway, responsible for nutrient and protein recycling, metabolism, response to infection, and external cell stresses. During autophagy, regulatory proteins organize an isolation membrane that develops into an autophagosome and then orchestrate its fusion with a lysosome. This pathway functions to proteolytic breakdown of cellular proteins and pathogens. The finding that cytokine-activated autophagosome synthesis did not match the levels of degradation suggests a "fractionated" autophagy response to Th2 cytokines. The portion of cytokine-activated autophagosome formation not degraded suggests a non-canonical autophagy fate. Non-canonical autophagy uses autophagy proteins for vesicle trafficking or secretion independent of autophagosome degradation [9–11,13,22]. Relevant to our findings, it was reported that in gut epithelium NADPH oxidase, NOX2, function and localization is dependent on vesicle trafficking to the autophagosome-amphisome [12]. In our data, the failure of DUOX1 to move to the apical membrane was associated with decrease superoxide levels in response to IL-13. An interpretation of our findings is that autophagy transports DUOX1 protein in a similar fashion to NOX2 [12] in the gut epithelium *via* endosome trafficking. Immunostaining revealed that LC3B does not closely associate with DUOX1 in the cytoplasm. Indeed, DUOX1 levels were not affected by genetic depletion of autophagy protein, ATG5. This finding supports, that autophagy does not control ROS levels by degrading DUOX1 in the lysosome.

There are potential limitations to these findings related to our use of reductionist models of epithelial cell activation rather than injury. *In vivo* we used the OVA-alum allergen challenge, a well-established model of Th2 type inflammation to demonstrate that autophagy is activated in the airway epithelium. In contrast to alternative allergen models, such as inhaled *Alternaria alternata* or house dust mice, the OVA-alum model is primarily a T cell-driven IL-13 and IL-4 response that relies less on direct epithelial cell damage and IL-33 release. This allowed us to focus on the direct role of Th2 cytokines, IL-13 and IL-4 rather than epithelial injury. Likewise, our *in vitro* models used only cytokine treatment to avoid autophagy responses that are shown to occur after airway epithelial infection [63]. The source of the Th2 cytokine-activated superoxide is presumed to be DUOX1 based on expression pattern *in vivo* and *in vitro*. Furthermore, inhibition of DUOX1 by siRNA did reduce intracellular superoxide levels. However, our data relies on indirect evidence that is contrary to the function of DUOX1. Biochemically, DUOX1 principally generates hydrogen peroxide through the intra-molecular dismutation of superoxide [32]. The addition of catalase to the apical cell surface failed to reduce intracellular superoxide. This suggests that apical extracellular hydrogen peroxide does not mediate the increase in intracellular superoxide. Future studies are needed to better understand the precise mechanisms by which Th2 cytokine-induced DUOX1 activity results in an increase in intracellular superoxide

In conclusion, our studies point to the airway epithelial cells as the source of significant superoxide generation *via* autophagy-directed DUOX1 localization. Treatment of airway epithelial cells by prolonged exposures to IL-13 and IL-4 activates an autophagy program that is required for both the generation of ROS and the proper intracellular localization of DUOX1. The specific factors associated with DUOX1 at the apical membrane that are required for increased intracellular superoxide levels are unknown, but are likely a component of the chronic inflammatory response in airway disease. These findings further implicate DUOX1 in disease pathogenesis and may serve as for targeted therapeutic interventions.

Acknowledgements

We thank Sean Gunsten for assistance with primary cell culture, Elizabeth Staab for assistance with the OVA challenged mouse model, and Jeff Haspel for his helpful comments. This work was supported by NIH Grants 1K08HL131992-01 (JDD) and R01HL122585 (SLB) and the Hubert C. and Dorothy R. Moog Professorship (SLB). EPR Spectroscopy data was collected in the University of Nebraska's EPR Spectroscopy Core, which is supported, in part, by a NIH grant from the National Institute of General Medical Sciences of the (P30GM103335) awarded to the University of Nebraska's Redox Biology Center.

Appendix A. Supplementary material

Supplementary data associated with this article can be found in the online version at http://dx.doi.org/10.1016/j.redox.2017.09.013.

References

[1] G. Bellot, R. Garcia-Medina, P. Gounon, J. Chiche, D. Roux, J. Pouyssegur, N.M. Mazure, Hypoxia-induced autophagy is mediated through hypoxia-inducible factor induction of BNIP3 and BNIP3L via their BH3 domains, Mol. Cell Biol. 29 (2009) 2570–2581.
[2] H.M. Wu, Z.F. Jiang, P.S. Ding, L.J. Shao, R.Y. Liu, Hypoxia-induced autophagy mediates cisplatin resistance in lung cancer cells, Sci. Rep. 5 (2015) 12291.
[3] A. Aguirre, I. Lopez-Alonso, A. Gonzalez-Lopez, L. Amado-Rodriguez, E. Batalla-Solis, A. Astudillo, J. Blazquez-Prieto, A.F. Fernandez, J.A. Galvan, C.C. dos Santos, et al., Defective autophagy impairs ATF3 activity and worsens lung injury during endotoxemia, J. Mol. Med. 92 (2014) 665–676.
[4] S. Li, L. Guo, P. Qian, Y. Zhao, A. Liu, F. Ji, L. Chen, X. Wu, G. Qian, Lipopolysaccharide induces autophagic cell death through the PERK-dependent branch of the unfolded protein response in human alveolar epithelial A549 cells, Cell Physiol. Biochem. 36 (2015) 2403–2417.
[5] J. Harris, Autophagy and cytokines, Cytokine 56 (2011) 140–144.
[6] Z.H. Chen, H.P. Kim, F.C. Sciurba, S.J. Lee, C. Feghali-Bostwick, D.B. Stolz, R. Dhir, R.J. Landreneau, M.J. Schuchert, S.A. Yousem, et al., Egr-1 regulates autophagy in cigarette smoke-induced chronic obstructive pulmonary disease, PLoS One 3 (2008) e3316.
[7] Z.H. Chen, H.C. Lam, Y. Jin, H.P. Kim, J. Cao, S.J. Lee, E. Ifedigbo, H. Parameswaran, S.W. Ryter, A.M. Choi, Autophagy protein microtubule-associated protein 1 light chain-3B (LC3B) activates extrinsic apoptosis during cigarette smoke-induced emphysema, Proc. Natl. Acad. Sci. USA 107 (2010) 18880–18885.
[8] H.P. Kim, X. Wang, Z.H. Chen, S.J. Lee, M.H. Huang, Y. Wang, S.W. Ryter, A.M. Choi, Autophagic proteins regulate cigarette smoke-induced apoptosis: protective role of heme oxygenase-1, Autophagy 4 (2008) 887–895.
[9] H. Farhan, M. Kundu, S. Ferro-Novick, The link between autophagy and secretion: a

story of multitasking proteins, Mol. Biol. Cell 28 (2017) 1161–1164.
[10] S. Davis, J. Wang, S. Ferro-Novick, Crosstalk between the secretory and autophagy pathways regulates autophagosome formation, Dev. Cell 41 (2017) 23–32.
[11] J. Wang, S. Davis, M. Zhu, E.A. Miller, S. Ferro-Novick, Autophagosome formation: where the secretory and autophagy pathways meet, Autophagy 13 (2017) 973–974.
[12] K.K. Patel, H. Miyoshi, W.L. Beatty, R.D. Head, N.P. Malvin, K. Cadwell, J.L. Guan, T. Saitoh, S. Akira, P.O. Seglen, et al., Autophagy proteins control goblet cell function by potentiating reactive oxygen species production, EMBO J. 32 (2013) 3130–3144.
[13] K. Moreau, M. Renna, D.C. Rubinsztein, Connections between SNAREs and autophagy, Trends Biochem. Sci. 38 (2013) 57–63.
[14] R. Scherz-Shouval, E. Shvets, E. Fass, H. Shorer, L. Gil, Z. Elazar, Reactive oxygen species are essential for autophagy and specifically regulate the activity of Atg4, EMBO J. 26 (2007) 1749–1760.
[15] R. Scherz-Shouval, Z. Elazar, ROS, mitochondria and the regulation of autophagy, Trends Cell Biol. 17 (2007) 422–427.
[16] R. Scherz-Shouval, Z. Elazar, Regulation of autophagy by ROS: physiology and pathology, Trends Biochem Sci. 36 (2011) 30–38.
[17] G. Filomeni, D. De Zio, F. Cecconi, Oxidative stress and autophagy: the clash between damage and metabolic needs, Cell Death Differ. 22 (2015) 377–388.
[18] I.H. Cho, Y.J. Choi, J.H. Gong, D. Shin, M.K. Kang, Y.H. Kang, Astragalin inhibits autophagy-associated airway epithelial fibrosis, Respir. Res. 16 (2015) 51.
[19] S.J. Lee, S.W. Ryter, J.F. Xu, K. Nakahira, H.P. Kim, A.M. Choi, Y.S. Kim, Carbon monoxide activates autophagy via mitochondrial reactive oxygen species formation, Am. J. Respir. Cell Mol. Biol. 45 (2011) 867–873.
[20] Y. Chen, M.B. Azad, S.B. Gibson, Superoxide is the major reactive oxygen species regulating autophagy, Cell Death Differ. 16 (2009) 1040–1052.
[21] J.D. Dickinson, Y. Alevy, N.P. Malvin, K.K. Patel, S.P. Gunsten, M.J. Holtzman, T.S. Stappenbeck, S.L. Brody, IL13 activates autophagy to regulate secretion in airway epithelial cells, Autophagy 12 (2016) 397–409.
[22] N. Martinez-Martin, P. Maldonado, F. Gasparrini, B. Frederico, S. Aggarwal, M. Gaya, C. Tsui, M. Burbage, S.J. Keppler, B. Montaner, et al., A switch from canonical to noncanonical autophagy shapes B cell responses, Science 355 (2017) 641–647.
[23] K. Dabbagh, K. Takeyama, H.M. Lee, I.F. Ueki, J.A. Lausier, J.A. Nadel, IL-4 induces mucin gene expression and goblet cell metaplasia in vitro and in vivo, J. Immunol. 162 (1999) 6233–6237.
[24] D.A. Kuperman, R.P. Schleimer, Interleukin-4, interleukin-13, signal transducer and activator of transcription factor 6, and allergic asthma, Curr. Mol. Med. 8 (2008) 384–392.
[25] M. Wills-Karp, J. Luyimbazi, X. Xu, B. Schofield, T.Y. Neben, C.L. Karp, D.D. Donaldson, Interleukin-13: central mediator of allergic asthma, Science 282 (1998) 2258–2261.
[26] Y.G. Alevy, A.C. Patel, A.G. Romero, D.A. Patel, J. Tucker, W.T. Roswit, C.A. Miller, R.F. Heier, D.E. Byers, T.J. Brett, et al., IL-13-induced airway mucus production is attenuated by MAPK13 inhibition, J. Clin. Investig. 122 (2012) 4555–4568.
[27] W.J. Calhoun, H.E. Reed, D.R. Moest, C.A. Stevens, Enhanced superoxide production by alveolar macrophages and air-space cells, airway inflammation, and alveolar macrophage density changes after segmental antigen bronchoprovocation in allergic subjects, Am. Rev. Respir. Dis. 145 (1992) 317–325.
[28] R. Forteza, M. Salathe, F. Miot, R. Forteza, G.E. Conner, Regulated hydrogen peroxide production by Duox in human airway epithelial cells, Am. J. Respir. Cell Mol. Biol. 32 (2005) 462–469.
[29] X. De Deken, D. Wang, M.C. Many, S. Costagliola, F. Libert, G. Vassart, J.E. Dumont, F. Miot, Cloning of two human thyroid cDNAs encoding new members of the NADPH oxidase family, J. Biol. Chem. 275 (2000) 23227–23233.
[30] S. Luxen, D. Noack, M. Frausto, S. Davanture, B.E. Torbett, U.G. Knaus, Heterodimerization controls localization of Duox-DuoxA NADPH oxidases in airway cells, J. Cell Sci. 122 (2009) 1238–1247.
[31] H. Grasberger, S. Refetoff, Identification of the maturation factor for dual oxidase. Evolution of an eukaryotic operon equivalent, J. Biol. Chem. 281 (2006) 18269–18272.
[32] T. Ueyama, M. Sakuma, Y. Ninoyu, T. Hamada, C. Dupuy, M. Geiszt, T.L. Leto, N. Saito, The extracellular A-loop of dual oxidases affects the specificity of reactive oxygen species release, J. Biol. Chem. 290 (2015) 6495–6506.
[33] M. Strengert, R. Jennings, S. Davanture, P. Hayes, G. Gabriel, U.G. Knaus, Mucosal reactive oxygen species are required for antiviral response: role of Duox in influenza a virus infection, Antioxid. Redox Signal. 20 (2014) 2695–2709.
[34] X. De Deken, B. Corvilain, J.E. Dumont, F. Miot, Roles of DUOX-mediated hydrogen peroxide in metabolism, host defense, and signaling, Antioxid. Redox Signal. 20 (2014) 2776–2793.
[35] P. Moskwa, D. Lorentzen, K.J. Excoffon, J. Zabner, P.B. McCray Jr., W.M. Nauseef, C. Dupuy, B. Banfi, A novel host defense system of airways is defective in cystic fibrosis, Am. J. Respir. Crit. Care Med. 175 (2007) 174–183.
[36] R.W. Harper, C. Xu, J.P. Eiserich, Y. Chen, C.Y. Kao, P. Thai, H. Setiadi, R. Wu, Differential regulation of dual NADPH oxidases/peroxidases, Duox1 and Duox2, by Th1 and Th2 cytokines in respiratory tract epithelium, FEBS Lett. 579 (2005) 4911–4917.
[37] S. Hirakawa, R. Saito, H. Ohara, R. Okuyama, S. Aiba, Dual oxidase 1 induced by Th2 cytokines promotes STAT6 phosphorylation via oxidative inactivation of protein tyrosine phosphatase 1B in human epidermal keratinocytes, J. Immunol. 186 (2011) 4762–4770.
[38] S. Chang, A. Linderholm, L. Franzi, N. Kenyon, H. Grasberger, R. Harper, Dual oxidase regulates neutrophil recruitment in allergic airways, Free Radic. Biol. Med. 65 (2013) 38–46.
[39] M. Hristova, A. Habibovic, C. Veith, Y.M. Janssen-Heininger, A.E. Dixon, M. Geiszt, A. van der Vliet, Airway epithelial dual oxidase 1 mediates allergen-induced IL-33 secretion and activation of type 2 immune responses, J. Allergy Clin. Immunol. 137 (2016) 1545–1556 (e11).
[40] A. Habibovic, M. Hristova, D.E. Heppner, K. Danyal, J.L. Ather, Y.M. Janssen-Heininger, C.G. Irvin, M.E. Poynter, L.K. Lundblad, A.E. Dixon, et al., DUOX1 mediates persistent epithelial EGFR activation, mucous cell metaplasia, and airway remodeling during allergic asthma, JCI Insight 1 (2016) e88811.
[41] Y. You, E.J. Richer, T. Huang, S.L. Brody, Growth and differentiation of mouse tracheal epithelial cells: selection of a proliferative population, Am. J. Physiol. Lung Cell Mol. Physiol. 283 (2002) L1315–L1321.
[42] A. Horani, A. Nath, M.G. Wasserman, T. Huang, S.L. Brody, Rho-associated protein kinase inhibition enhances airway epithelial Basal-cell proliferation and lentivirus transduction, Am. J. Respir. Cell Mol. Biol. 49 (2013) 341–347.
[43] S.V. Costes, D. Daelemans, E.H. Cho, Z. Dobbin, G. Pavlakis, S. Lockett, Automatic and quantitative measurement of protein-protein colocalization in live cells, Biophys. J. 86 (2004) 3993–4003.
[44] D.J. Klionsky, K. Abdelmohsen, A. Abe, M.J. Abedin, H. Abeliovich, A. Acevedo Arozena, H. Adachi, C.M. Adams, P.D. Adams, K. Adeli, et al., Guidelines for the use and interpretation of assays for monitoring autophagy (3rd edition), Autophagy 12 (2016) 1–222.
[45] A.J. Case, C.T. Roessner, J. Tian, M.C. Zimmerman, Mitochondrial superoxide signaling contributes to norepinephrine-mediated T-Lymphocyte cytokine profiles, PLoS One 11 (2016) e0164609.
[46] A.J. Case, S. Li, U. Basu, J. Tian, M.C. Zimmerman, Mitochondrial-localized NADPH oxidase 4 is a source of superoxide in angiotensin II-stimulated neurons, Am. J. Physiol. Heart Circ. Physiol. 305 (2013) H19–H28.
[47] W.H. Wan, F. Hollins, L. Haste, L. Woodman, R.A. Hirst, S. Bolton, E. Gomez, A. Sutcliffe, D. Desai, L. Chachi, et al., NADPH oxidase 4 over-expression is associated with epithelial ciliary dysfunction in neutrophilic asthma, Chest (2016).
[48] S.A. Comhair, P.R. Bhathena, R.A. Dweik, M. Kavuru, S.C. Erzurum, Rapid loss of superoxide dismutase activity during antigen-induced asthmatic response, Lancet 355 (2000) 624.
[49] S.A. Comhair, W. Xu, S. Ghosh, F.B. Thunnissen, A. Almasan, W.J. Calhoun, A.J. Janocha, L. Zheng, S.L. Hazen, S.C. Erzurum, Superoxide dismutase inactivation in pathophysiology of asthmatic airway remodeling and reactivity, Am. J. Pathol. 166 (2005) 663–674.
[50] H.R. De Raeve, F.B. Thunnissen, F.T. Kaneko, F.H. Guo, M. Lewis, M.S. Kavuru, M. Secic, M.J. Thomassen, S.C. Erzurum, Decreased Cu,Zn-SOD activity in asthmatic airway epithelium: correction by inhaled corticosteroid in vivo, Am. J. Physiol. 272 (1997) L148–L154.
[51] X.T. Wang, J. Zhou, B.L. Lei, J.M. Zhou, S.Y. Xu, B.P. Hu, D.Q. Wang, D.P. Zhang, M.H. Wu, Atmospheric occurrence, homologue patterns and source apportionment of short- and medium-chain chlorinated paraffins in Shanghai, China: biomonitoring with Masson pine (Pinus massoniana L.) needles, Sci. Total Environ. 560–561 (2016) 92–100.
[52] D.E. Byers, J. Alexander-Brett, A.C. Patel, E. Agapov, G. Dang-Vu, X. Jin, K. Wu, Y. You, Y. Alevy, J.P. Girard, et al., Long-term IL-33-producing epithelial progenitor cells in chronic obstructive lung disease, J. Clin. Investig. 123 (2013) 3967–3982.
[53] S.A. Comhair, S.C. Erzurum, Redox control of asthma: molecular mechanisms and therapeutic opportunities, Antioxid. Redox Signal. 12 (2010) 93–124.
[54] H.J. Forman, O. Augusto, R. Brigelius-Flohe, P.A. Dennery, B. Kalyanaraman, H. Ischiropoulos, G.E. Mann, R. Radi, L. Jackson Roberts 2nd, J. Vina, et al., Even free radicals should follow some rules: a suggested guide to free radical research terminology and methodology, Free Radic. Biol. Med (2014).
[55] S.H. Gorissen, M. Hristova, A. Habibovic, L.M. Sipsey, P.C. Spiess, Y.M. Janssen-Heininger, A. van der Vliet, Dual oxidase-1 is required for airway epithelial cell migration and bronchiolar reepithelialization after injury, Am. J. Respir. Cell Mol. Biol. 48 (2013) 337–345.
[56] M.X. Shao, J.A. Nadel, Dual oxidase 1-dependent MUC5AC mucin expression in cultured human airway epithelial cells, Proc. Natl. Acad. Sci. USA 102 (2005) 767–772.
[57] A. Luciani, V.R. Villella, S. Esposito, N. Brunetti-Pierri, D.L. Medina, C. Settembre, M. Gavina, V. Raia, A. Ballabio, L. Maiuri, Cystic fibrosis: a disorder with defective autophagy, Autophagy 7 (2011) 104–106.
[58] A. Luciani, V.R. Villella, S. Esposito, N. Brunetti-Pierri, D. Medina, C. Settembre, M. Gavina, L. Pulze, I. Giardino, M. Pettoello-Mantovani, et al., Defective CFTR induces aggresome formation and lung inflammation in cystic fibrosis through ROS-mediated autophagy inhibition, Nat. Cell Biol. 12 (2010) 863–875.
[59] H.C. Lam, S.M. Cloonan, A.R. Bhashyam, J.A. Haspel, A. Singh, J.F. Sathirapongsasuti, M. Cervo, H. Yao, A.L. Chung, K. Mizumura, et al., Histone deacetylase 6-mediated selective autophagy regulates COPD-associated cilia dysfunction, J. Clin. Investig. 123 (2013) 5212–5230.
[60] K. Nakahira, S.M. Cloonan, K. Mizumura, A.M. Choi, S.W. Ryter, Autophagy: a crucial moderator of redox balance, inflammation, and apoptosis in lung disease, Antioxid. Redox Signal. 20 (2014) 474–494.
[61] Y. Chen, E. McMillan-Ward, J. Kong, S.J. Israels, S.B. Gibson, Oxidative stress induces autophagic cell death independent of apoptosis in transformed and cancer cells, Cell Death Differ. 15 (2008) 171–182.
[62] J.L. Barlow, S. Peel, J. Fox, V. Panova, C.S. Hardman, A. Camelo, C. Bucks, X. Wu, C.M. Kane, D.R. Neill, et al., IL-33 is more potent than IL-25 in provoking IL-13-producing nuocytes (type 2 innate lymphoid cells) and airway contraction, J. Allergy Clin. Immunol. 132 (2013) 933–941.
[63] D.R. Hahn, C.L. Na, T.E. Weaver, Reserve autophagic capacity in alveolar epithelia provides a replicative niche for influenza A virus, Am. J. Respir. Cell Mol. Biol. (2014).